Supplement of

Magnetic Fabric Analyses of Basin Inversion: A Sandbox Modelling approach

Thorben Schöfisch et al.

Correspondence to: Thorben Schöfisch (thorben.schofisch@geo.uu.se)

List of figures and tables

- Figure S1. Pictures with structural measurements showing narrowing of basins during inversion.
- Figure S2. Calculation of structure-to-sample size ratio for samples taken at faults.

- Table 1. Calculation of layer length during basin inversion.

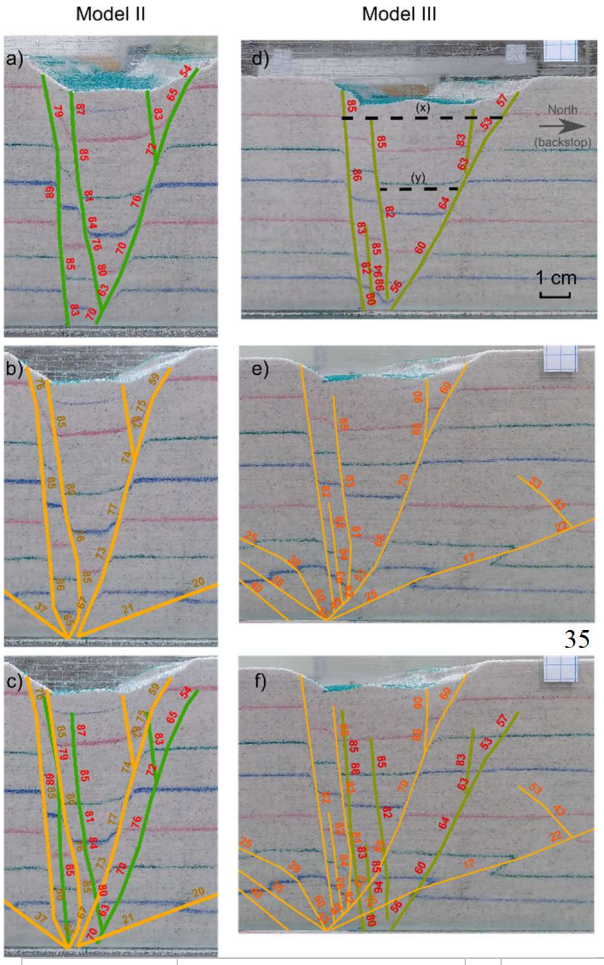

Figure S1: Excerpt from sideview through glass wall of basin area of inverted basin models II and III at different stages. Structural measurements (inclination of fault segments) are taken after model extension for basin area (a, b – faults in green with red inclination values in degree), and after model inversion (b, e – faults in orange with orange inclination values in degree). Both stages are compared in c) and f). It occurs that the normal faults that bound the basin are very steep and are modified with increasing model shortening. Significant changes are observed for the northern normal fault (vergence towards the backstop). These northern normal faults steepen with inversion, causing a basin narrowing that is calculated in Table 1. Moreover, the basins moved into direction of shortening (to the south) during inversion.

	Model II			Model III	
Layer	dx [mm]	dy [mm]		dx [mm]	dy [mm]
1 – red	-2.5	-0.4		-3.5	-1.6
2 – green	-1.7	-0.8		-2.8	-0.8
3 – blue	-1.6	-0.1		-3.6	-0.3
4 – red	-2.1	-0.3		-2.7	-0.9
5 – green	-1.6	-1.5		-2.4	-0.5

Table 1: Two differences in layer length (dx and dy) between the length before and after inversion are calculated for models II and III. dx is the difference between the two model stages using the horizontal distance connecting the same layer in each footwall on each side of the basin, i.e., the intersections of the layer with the normal faults is used as reference. dy represents the difference in horizontal length of a layer within the basin/hangingwall between the two model stages (i.e., before and after inversion). In conclusion, the two differences (dx and dy) show a basin narrowing after inversion. The basin narrowing is very small and including a potential error estimation due to image referencing would undermine the results. However, changes in width of the basin is identified in both inverted models.

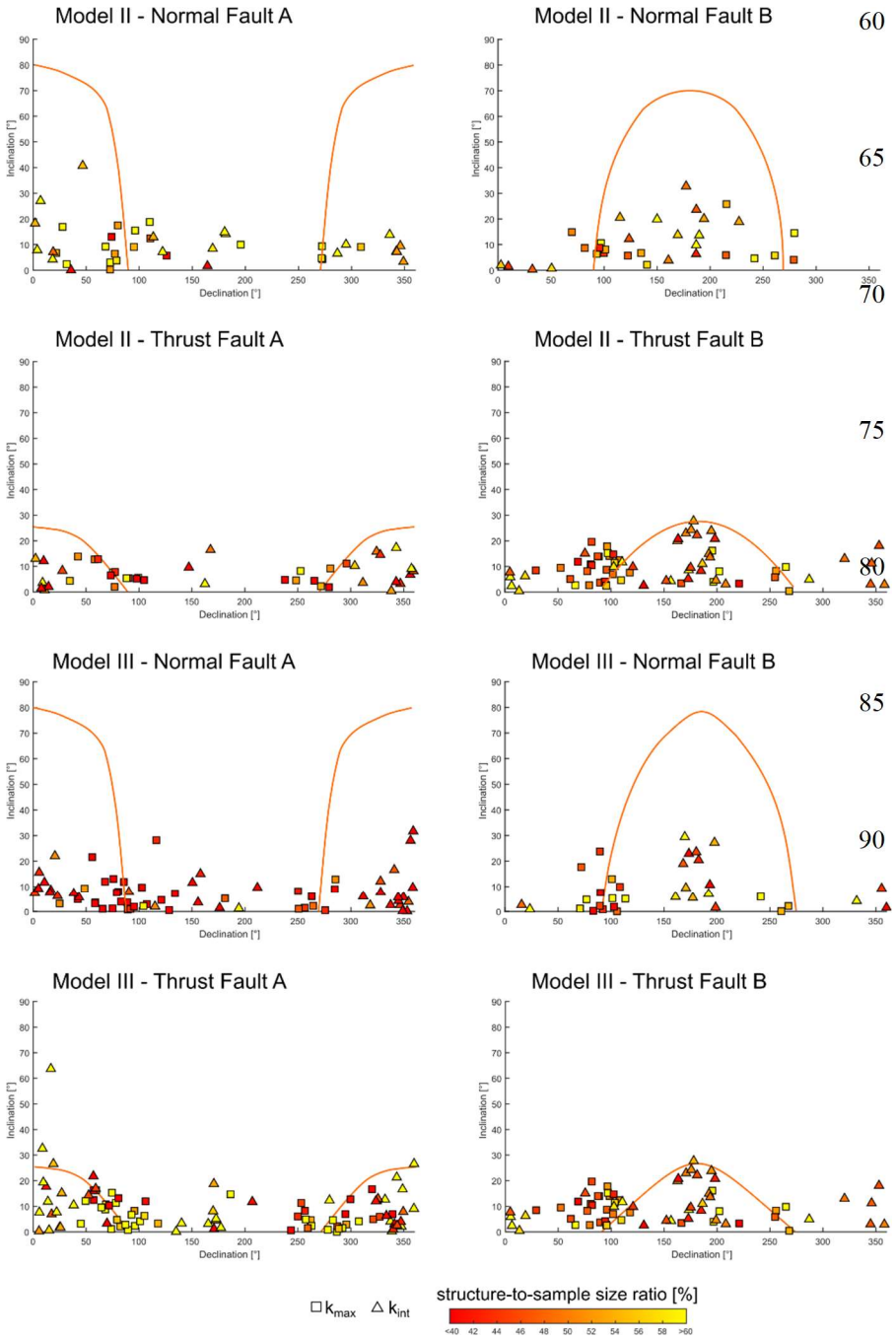

Figure S2: The declination is plotted against the inclination of the k_{max} (squares) and k_{int} axes (triangles) for the normal faults and thrust faults of models II and III. The colormap (from red to yellow) of the symbols gives information of how much of the structure/fault is within a sample, i.e., dimension of the shear zone compared to the area that is not affected by the fault within one sample container (structure-to-sample size ratio in %). The k_{max} and k_{int} axes define a magnetic foliation that aligns parallel to the fault surface during shearing. The orientations of the fault surfaces are represented with the orange lines. In general, the k_{max} and k_{int} axes display a greater alignment with thrust as with normal fault surfaces. Moreover, it can be discussed that as more structure (yellowish colours) is captured within a sample as greater is the alignment of the magnetic foliation with the fault surface. However, this is not completely true for the complete datasets and exceptions need to be investigated. Such investigation is beyond this study and the authors suggest further studies for an improved understanding of the effect of sampling/sample size in magnetic fabric analyses of sandbox models.